

# Discrimination between glioma grades II and III in suspected low-grade gliomas using dynamic contrast-enhanced and dynamic susceptibility contrast perfusion MR imaging: a histogram analysis approach

Anna Falk · Markus Fahlström · Egill Rostrup ·  
Shala Berntsson · Maria Zetterling · Arvid Morell ·  
Henrik B.W. Larsson · Anja Smits · Elna-Marie Larsson

Received: 9 July 2014 / Accepted: 26 August 2014 / Published online: 10 September 2014  
© Springer-Verlag Berlin Heidelberg 2014

## Abstract

**Introduction** Perfusion magnetic resonance imaging (MRI) can be used in the pre-operative assessment of brain tumours. The aim of this prospective study was to identify the perfusion parameters from dynamic contrast-enhanced (DCE) and dynamic susceptibility contrast (DSC) perfusion imaging that could best discriminate between grade II and III gliomas.

**Methods** MRI (3 T) including morphological ((T2 fluid attenuated inversion recovery (FLAIR) and T1-weighted (T1W)+Gd)) and perfusion (DCE and DSC) sequences was performed in 39 patients with newly diagnosed suspected low-grade glioma after written informed consent in this review board-approved study. Regions of interests (ROIs) in tumour area were delineated on FLAIR images co-registered to DCE and DSC, respectively, in 25 patients with histopathological grade II ( $n=18$ ) and III ( $n=7$ ) gliomas. Statistical analysis of differences between grade II and grade III gliomas in histogram perfusion parameters was performed, and the areas under the curves (AUC) from the ROC analyses were evaluated.

**Results** In DCE, the skewness of transfer constant ( $k_{\text{trans}}$ ) was found superior for differentiating grade II from grade III in all

gliomas (AUC 0.76). In DSC, the standard deviation of relative cerebral blood flow (rCBF) was found superior for differentiating grade II from grade III gliomas (AUC 0.80).

**Conclusions** Histogram parameters from  $k_{\text{trans}}$  (DCE) and rCBF (DSC) could most efficiently discriminate between grade II and grade III gliomas.

**Keywords** Dynamic contrast-enhanced MRI · Dynamic susceptibility contrast MRI · Perfusion MRI · Glioma · Histogram analysis

## Abbreviations

AUC	Area under the curve
DCE	Dynamic contrast-enhanced
DSC	Dynamic susceptibility contrast
FLAIR	Fluid attenuated inversion recovery
ICA	Internal carotid artery
$k_{\text{trans}}$	Transfer constant
$K_{\text{app}}$	Apparent transfer constant
ROI	Region of interest
ROC	Receiver operating characteristics
T1W	T1-weighted
TE	Echo time
TR	Repetition time

Elna-Marie Larsson and Anja Smits share senior authorship.

A. Falk (✉) · M. Fahlström · A. Morell · E.-M. Larsson  
Department of Radiology, Oncology and Radiation Science,  
Section of Radiology, Uppsala University, BFC Akademiska  
sjukhuset, SE 751 85 Uppsala, Sweden  
e-mail: aka03nfa@gmail.com

E. Rostrup · H. B. Larsson  
Functional Imaging Unit, Glostrup Hospital, Glostrup, University of  
Copenhagen, Copenhagen, Denmark

S. Berntsson · M. Zetterling · A. Smits  
Department of Neuroscience, Neurology, Uppsala University,  
Uppsala, Sweden

## Background and purpose

Gliomas are glial tumours of the central nervous system that are diagnosed according to the World Health Organization classification of brain tumours [1]. Grade I and II gliomas are considered low-grade, whereas grade III and IV gliomas (glioblastomas) are considered high-grade. Gliomas are

classified by cell type and occur mainly as astrocytomas, oligodendrogliomas or oligoastrocytomas, a mixed form with both oligodendroglial and astrocytic components [2, 3]. In adults, low-grade gliomas consist of grade II gliomas. These are slowly proliferating tumours that display cytological atypia but no signs of anaplasia, endothelial cell proliferation or brisk mitotic activity [1].

An assessment of tumour malignancy grade in the pre-operative situation is important for clinical management, especially for tumours in eloquent areas when maximal tumour resection must be balanced by preservation of neurological function. Magnetic resonance imaging (MRI) is the method of choice for the radiological evaluation of brain tumours. However, discriminating low-grade from high-grade gliomas by conventional morphological MRI has been difficult [4]. Whilst glioblastomas usually exhibit characteristic contrast enhancement, overlapping contrast enhancement patterns occur between grade II and III gliomas. Dynamic susceptibility contrast (DSC) perfusion imaging and dynamic contrast-enhanced (DCE) perfusion imaging are two perfusion MRI methods based on intravenous contrast agent injection that can be used in the assessment of tumour malignancy grade and physiology [5, 6]. DSC is the most commonly used perfusion MRI technique in neuroradiological practice. In DSC, susceptibility effects from the contrast agent result in magnetic field inhomogeneity, causing a drop in signal during the contrast bolus passage through the capillary bed. A T2\*W gradient echo sequence with echo planar imaging (EPI) readout is used. DSC generates relative perfusion maps requiring normalisation with a normal appearing region because of the risk of errors in estimating the arterial input function [7, 8]. DSC is thus not used for absolute quantification of cerebral perfusion [5].

In DCE, bolus contrast agent passage yields a signal increase on a T1-weighted gradient echo sequence due to T1 shortening. DCE allows for absolute quantification of perfusion parameters and is not disturbed by susceptibility artefacts [9–11].

Earlier efforts to discriminate low-grade from high-grade gliomas have mainly focused on tumours with an astrocytic phenotype [12–15]. The maximal cerebral blood volume within a region ( $CBV_{max}$ ) has been shown to reflect neo-vascularisation and correlate with the malignancy grade of astrocytomas [13]. Astrocytomas and oligodendrogliomas differ, however, in vascular density and thereby also in cerebral blood volume (CBV), complicating the pre-operative evaluation by perfusion MRI when tumour cell type is still unknown [6]. The discrimination of grade II gliomas from grade III gliomas in a population of mixed tumour types has been proven to be challenging [15–18]. In addition, perfusion parameters other than CBV have not been studied extensively.

The aim of the present study was to identify perfusion parameters from DCE and DSC perfusion studies that could best discriminate grade II from grade III gliomas.

## Materials and methods

### Patient characteristics

Thirty-nine patients with clinical and radiological suspected low-grade glioma, referred to the neurosurgical department between May 2010 and November 2012, were prospectively and consecutively recruited [19]. The institutional review board approved the study protocol, and all patient participation was based on written informed consent. An intracerebral tumour-suspected lesion on morphological MRI with high signal intensity on T2 fluid attenuated inversion recovery (FLAIR) and with no or minimal contrast enhancement was regarded as a suspected low-grade glioma (assessed by a neuroradiologist with 30 years of experience). Exclusion criteria for the present study were other histological diagnosis than grade II or grade III glioma ( $n=4$ ), no histologically diagnosis available ( $n=8$ ) or obtained more than 12 months after the study MRI ( $n=2$ ). Thus, 25 patients with grade II or grade III glioma were enrolled in the present study. The clinical characteristics of these 25 patients are shown in Table 1. The study MRI was performed pre-operatively in all but one patient. This patient (patient 2) had a biopsy performed 6 months prior to the study MRI.

### MRI

Imaging was performed on a 3-T MRI scanner with a 32-channel head coil (Achieva, Philips Healthcare, Best, the Netherlands) and included morphological and perfusion sequences.

*Morphological MRI* included axial T2 FLAIR (repetition time (TR)/echo time (TE) 11,000/125 ms; 90° flip angle; 512×512 matrix; 0.45×0.45×6 mm<sup>3</sup> voxel size) and T1W spin echo sequences after intravenous contrast agent administration (TR/TE 600/10 ms; 70° flip angle; 512×512 matrix; 0.45×0.45×5 mm<sup>3</sup> voxel size).

### Perfusion MRI

DCE was performed with a T1W-spoiled saturation recovery gradient echo sequence covering four slices over the centre of the tumour and one slice perpendicular to the internal carotid artery for arterial input function determination. The following parameters were used: temporal resolution 1.25 s; time delay between the prepulse and the first readout pulse 120 ms, TR/TE 3.97/1.9 ms; flip angle 30°; acquired voxel size 2.4×3.0×8.0 mm<sup>3</sup>; and matrix 256×256. A total of ten dynamic scans were performed before the intravenous injection of 0.05 mmol/kg gadolinium-based contrast agent (gadobutrol 1 mmol/mL) at 3 mL/s, followed by a 30-mL saline injection at the same injection rate, using a power injector. Total acquisition time was 5 min with 200 dynamic scans.

**Table 1** Patient characteristics

Patient	Patient age at MRI (years)	Contrast enhancement	Tumour type	Tumour grade	Time between MRI and histology (months)	Biopsy or resection (%)
1	62	None	Oligoastrocytoma	II	10	Resection (approx 50 %)
2	66	Yes, homogenous, diffuse	Astrocytoma	III	6	Needle biopsy
3	40	None	Oligodendroglioma	II	<1	Resection (approx 50 %)
4	28	None	Oligoastrocytoma	III	<1	Resection (approx 25 %)
5	31	Yes, patchy, diffuse	Oligoastrocytoma	III	<1	Resection (approx 25 %)
6	36	None	Astrocytoma	III	2	Needle biopsy
7	31	Yes, diffuse	Oligodendroglioma	II	<1	Resection (approx 50 %)
8	42	None	Oligodendroglioma	II	4	Resection (approx 75 %)
9	25	None	Oligodendroglioma	II	1	Resection (>90 %)
10	79	None	Astrocytoma	III	3	Resection (>90 %)
11	55	None	Astrocytoma	II	<1	Needle biopsy
12	63	None	Astrocytoma	II	<1	Needle biopsy
13	22	None	Oligoastrocytoma	II	<1	Resection (approx 40 %)
14	70	Yes, patchy, diffuse	Astrocytoma	III	<1	Open biopsy
15	41	None	Oligodendroglioma	III	1	Resection (approx 50 %)
16	53	None	Oligoastrocytoma	II	3	Total resection
17	41	None	Oligoastrocytoma	II	3	Resection (approx 50 %)
18	44	None	Astrocytoma	II	<1	Open biopsy
19	68	None	Astrocytoma	II	<1	Open biopsy
20	44	None	Oligodendroglioma	II	<1	Resection (approx 50 %)
21	66	None	Astrocytoma	II	3	Resection (approx 30 %)
22	34	Discrete	Oligoastrocytoma	II	2	Resection (approx 90 %)
23	61	None	Astrocytoma	II	2	Resection (approx 90 %)
24	54	None	Oligodendroglioma	II	4	Resection (approx 30 %)
25	33	None	Oligodendroglioma	II	<1	Total resection

Post-processing was performed in MatLab (MathWorks, Natick, MA), using an in-house developed semi-automatic procedure. Briefly, regions of interests (ROIs) delineating internal carotid artery (ICA) and the superior sagittal sinus were drawn. In order to minimise partial volume effect, the arterial input function was derived from the one voxel in the ICA with maximal signal change during contrast agent bolus passage. Correction for partial volume was performed by normalising the signal to a venous outflow function, derived from the superior sagittal sinus. Calculation of perfusion data and corresponding maps for CBV, cerebral blood flow (CBF) and transfer constant ( $k_{trans}$ ) [20] was performed according to a method described by Larsson et al. [10, 11].

DSC was performed, 10 min after DCE, with a T2\*W single shot gradient echo-EPI sequence covering 23 slices with the following parameters: temporal resolution 1.35 s; echo time 29 ms; flip angle 90°; acquired voxel size  $1.7 \times 2.3 \times 5.0 \text{ mm}^3$ ; and matrix  $128 \times 128$ . Pre-contrast bolus scanning was performed during 10 s before intravenous injection of 5 mL gadolinium-based contrast agent (gadobutrol 1 mmol/mL) at 4 mL/s, followed by a 30-mL saline infusion

at the same rate, using a power injector. Total acquisition time was 90 s with 72 dynamic scans. Whole brain coverage was obtained using these parameters. Briefly, prior injection of contrast agent during DCE pre-saturated the tissue. Contrast agent leakage from the intravascular to the extravascular space was corrected for using the method published by Boxerman et al. [21], and this correction produces leakage maps where the pixel intensity is proportional to the rate of contrast agent leakage from the intra- to the extravascular space, referred to as the apparent transfer constant ( $K_{app}$ ). Motion correction was performed [22]. The arterial input function was measured from branches of the middle cerebral artery in the hemisphere contralateral to the tumour and inspected visually for a narrow peak. Calculation of perfusion data and corresponding maps of CBV, CBF and  $K_{app}$  [21] was performed using the software nordicICE (NordicNeuroLab AS, Bergen, Norway) with the Tikhonov regularisation method for deconvolution [23].

Axial FLAIR images were transferred to the same voxel space and co-registered to DCE and DSC images, respectively, using SPM8 (MathWorks, Natick, MA). All ROIs were manually delineated on the FLAIR images using an in-house

developed MatLab-based software and transferred to the perfusion maps (Fig. 1a, b). The tumour ROI was delineated just inside its border, on all slices with high FLAIR signal by a resident in radiology (3 years of experience) blinded to histopathological diagnosis. Tumour delineation was performed on all co-registered FLAIR slices with suspected tumour changes that had a corresponding perfusion slice on DCE and DSC, respectively. A ROI in the normal appearing white matter was delineated in the lobe contralateral to the tumour area in one slice.

Perfusion data from the ROIs were presented as histogram parameters of median, mean, standard deviation, kurtosis, skewness, peak position, peak height and the 90th percentile.

Histological tumour diagnosis was obtained by neuronavigation-guided needle biopsy ( $n=4$ ), open biopsy ( $n=3$ ) or resection ( $n=18$ ), as previously described [19]. Estimation of extent of resection was based on 48 h post-operatively MRI except in one case who had a post-operative CT and is presented in Table 1.

#### Statistical analysis

Statistical software Statistica 12 (Statsoft, Tulsa, OK, USA) was used for the analyses of perfusion data: CBV, CBF and  $k_{trans}$  from DCE and CBV, CBF and  $K_{app}$  from DSC. Normalisation against normal appearing contralateral white matter was performed for CBV and CBF histogram parameters mean, median, peak position and 90th percentile from DSC and DCE. Not normalised parameters were standard deviation, kurtosis, skewness, peak height and parameters from  $k_{trans}$  and  $K_{app}$ .

Data distribution was analysed by normal probability plot and Shapiro-Wilk's  $W$  test. Pairwise comparisons of perfusion parameters between tumour grade II and III were assessed in all gliomas ( $n=25$ ). A parametric Student's  $t$  test was applied for normally distributed data, and a non-parametric test

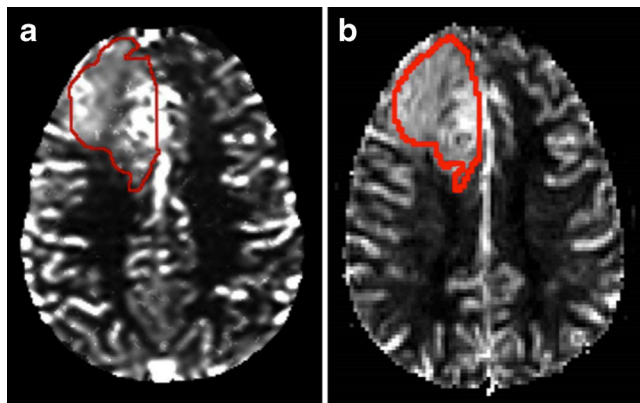


**Fig. 1** DCE (a) and DSC (b) perfusion in an oligodendroglioma grade II. The region of interest delineates the tumour border

(Mann–Whitney  $U$ ) was chosen for data that did not fulfil the requirements for normality.

Differences in perfusion parameters between grade II and III gliomas were further analysed using receiver operating characteristic (ROC) curves and comparing the area under the curve (AUC). The parameter with the highest AUC was presented as the best discriminating parameter.

## Results

#### Mean perfusion parameters in glioma grade II and grade III

DCE Mean $\pm$ SD rCBVp in glioma grade II was  $1.34\pm 0.37$  and  $1.82\pm 1.12$  in glioma grade III,  $p=0.65$ . Mean $\pm$ rCBF in glioma grade II was  $1.47\pm 0.54$  and  $1.85\pm 1.55$  in glioma grade III,  $p=0.79$ . Mean  $k_{trans}$  in glioma grade II was  $0.22\pm 0.30$  and  $0.26\pm 0.23$  in glioma grade III,  $p=0.32$ .

DSC Mean $\pm$ SD rCBV in glioma grade II was  $1.48\pm 0.74$  and  $2.42\pm 1.99$  in glioma grade III,  $p=0.21$ . Mean $\pm$ SD rCBF in glioma grade II was  $1.66\pm 0.99$  and  $2.53\pm 1.88$  in glioma grade III,  $p=0.24$ . Mean  $K_{app}$  in glioma grade II was  $33.54\pm 30.51$  and  $94.15\pm 78.10$  in glioma grade III,  $p=0.07$ .

#### Histogram analysis of perfusion parameters

Histogram parameters from the DCE and DSC perfusion scans were compared between grade II and III gliomas.

For DCE, the perfusion parameter skewness of  $k_{trans}$  had the lowest  $p$  value for separating glioma grades II and III ( $p=0.07$ ). Histogram perfusion parameters from DCE for glioma grades II and III are presented in Table 2.

For DSC, the standard deviation of CBF had the lowest  $p$  value and showed significant difference between glioma grade II and glioma grade III ( $p=0.02$ ). Histogram perfusion parameters from DSC for glioma grades II and III are presented in Table 3.

#### ROC curve analysis

ROC curves were analysed for glioma grades II and III ( $n=25$ ) with data from the DCE and DSC MRI perfusions (Tables 2 and 3). In DCE, the skewness of  $k_{trans}$  had the highest AUC (0.76) for separating between glioma grade II and glioma grade III (Fig. 2a).

In DSC, the standard deviation of CBF had the highest AUC (0.80) for separating between glioma grade II and glioma grade III (Fig. 2b).

**Table 2** Pairwise comparison between DCE perfusion parameters from histogram analysis in grade II and grade III glioma

			Glioma II <i>n</i> =18	Glioma III <i>n</i> =7	<i>p</i>	Test type	AUC
DCE	rCBVp	Mean	1.34±0.37	1.82±1.12	0.65	mw	0.56
		Median	1.18±0.33	1.66±1.25	0.69	mw	0.56
		Peak position	1.00±0.29	1.37±1.10	0.69	mw	0.56
		90th percentile	1.41±0.49	1.94±0.98	0.29	mw	0.64
	CBVp	Peak height	0.20±0.08	0.19±0.09	0.90	tt	0.53
		Standard deviation	1.60±0.76	1.89±1.02	0.93	mw	0.52
		Skewness	2.36±1.37	2.37±1.36	0.98	tt	0.50
		Kurtosis	12.22±15.34	10.89±8.77	0.93	mw	0.52
DCE	rCBF	Mean	1.47±0.54	1.85±1.55	0.79	mw	0.54
		Median	1.27±0.48	1.78±1.83	0.88	mw	0.52
		Peak position	1.19±0.46	2.01±3.44	0.08	mw	0.73
		90th percentile	1.59±0.72	1.93±1.30	0.88	mw	0.52
	CBF	Peak height	0.22±0.07	0.23±0.08	0.77	tt	0.60
		Standard deviation	21.41±14.56	19.11±12.17	0.65	mw	0.56
		Skewness	2.85±1.29	2.49±1.43	0.55	tt	0.56
		Kurtosis	14.57±13.00	12.57±13.36	0.61	mw	0.57
DCE	<i>k</i> <sub>trans</sub>	Mean	0.22±0.30	0.26±0.23	0.32	mw	0.64
		Median	0.15±0.23	0.18±0.17	0.38	mw	0.62
		Peak position	0.23±0.18	0.23±0.08	0.69	mw	0.56
		90th percentile	0.70±0.55	0.81±0.47	0.17	mw	0.68
		Peak height	0.52±0.18	0.51±0.13	0.90	tt	0.50
		Standard deviation	0.31±0.30	0.31±0.17	0.32	mw	0.64
		Skewness	<b>1.60±1.60</b>	<b>2.86±0.97</b>	<b>0.07</b>	<b>tt</b>	<b>0.76</b>
		Kurtosis	10.08±13.36	13.95±10.07	0.14	mw	0.70

The best discriminating parameter is presented in bold font

mw Mann–Whitney *U* test, tt Student's *t* test

## Discussion

There is a need for non-invasive parameters that can distinguish grade II from grade III tumours in patients with suspected low-grade gliomas on conventional MRI, to facilitate surgical treatment planning. MRI perfusion in patients with glioma has been studied with regard to pre-operative tumour grading [13, 15], and the CBV has been able to separate low-grade from high-grade astrocytomas [14, 24, 25]. However, the separation of glioma grade II from grade III is difficult due to overlapping features. Studies using MRI perfusion of oligodendrogliomas and mixed gliomas have shown ambiguous results [14–17, 26].

In this study, we identified the histogram perfusion parameter from DCE and DSC that could most efficiently discriminate between glioma grades II and III in a pre-operative situation when tumour cell type is unknown. The AUC from ROC analyses between glioma grade II and glioma grade III was highest for histogram parameters skewness of *k*<sub>trans</sub> (DCE) (AUC=0.76) and the standard deviation of CBF (DSC) (AUC=0.80).

Our results add new information to the few previously published reports on this topic. Cha et al. showed that *k*<sub>trans</sub> from MRI perfusion was superior to CBV for predicting malignancy grade in a cohort of 20 glioma grades I–IV [27]. Compared to the work by Cha et al., we analysed a larger group of glioma grades II and III (25 patients compared to 9).

Earlier MRI perfusion studies have used a small ROI approach analysing only a fraction of the whole tumour [13–15, 28]. We propose that the whole tumour analysis as used in this study better reflects the visual evaluation performed by the neuroradiologist in clinical practice when assessing the complete tumour area. Whole tumour analysis also evades the problematic interpretation of small areas of suspected aberrant perfusion that can be cumbersome to detect in perfusion MRI because of low spatial resolution, artefacts and partial volume effects. Such areas are especially difficult to assess correctly in low-grade gliomas with predominantly low perfusion. Whole tumour analysis therefore limits the inter-individual variations from interpretation and is probably a method that is easier to standardise and automatise.



**Table 3** Pairwise comparison between DSC perfusion parameters from histogram analysis in grade II and grade III glioma

			Glioma II <i>n</i> =18	Glioma III <i>n</i> =7	<i>p</i>	Test type	AUC
DSC	rCBV	Mean	1.48±0.74	2.42±1.99	0.21	mw	0.67
		Median	1.27±0.80	1.82±1.78	0.57	mw	0.58
		Peak position	1.06±0.66	1.43±2.04	0.53	mw	0.59
		90th percentile	<b>1.67±0.78</b>	<b>2.91±1.79</b>	<b>0.04</b>	<b>mw</b>	0.77
	CBV	Peak height	0.21±0.09	0.19±0.08	0.67	tt	0.56
		Standard deviation	176.22±90.34	263.40±192.10	0.29	mw	0.64
		Skewness	2.61±0.93	2.49±1.19	0.79	tt	0.55
		Kurtosis	11.77±7.72	14.16±17.01	0.83	mw	0.53
DSC	rCBF	Mean	1.66±0.99	2.53±1.88	0.24	mw	0.66
		Median	1.45±1.00	2.06±1.93	0.57	mw	0.58
		Peak position	1.27±0.88	2.97±5.90	0.35	mw	0.63
		90th percentile	1.84±0.98	2.96±1.91	0.06	mw	0.75
	CBF	Peak height	0.25±0.11	0.19±0.08	0.15	tt	0.68
		Standard deviation	<b>173.56±87.43</b>	<b>330.51±172.61</b>	<b>0.02</b>	<b>mw</b>	0.80
		Skewness	3.00±1.03	2.75±1.19	0.60	tt	0.54
		Kurtosis	14.55±9.07	14.47±12.84	0.93	mw	0.52
DSC	<i>K</i> <sub>app</sub>	Mean	33.54±30.51	94.15±78.10	0.07	mw	0.74
		Median	12.19±36.93	20.57±54.43	0.88	mw	0.52
		Peak position	0±0	18.95±50.14	0.61	mw	0.57
		90th percentile	142.91±66.40	238.24±124.25	0.08	mw	0.73
		Peak height	0.73±0.18	0.58±0.25	0.10	tt	0.70
		Standard deviation	97.40±37.78	151.26±108.52	0.57	mw	0.58
		Skewness	-1.92±4.38	0.56±1.91	0.11	mw	0.71
		Kurtosis	46.53±84.85	13.57±14.40	0.41	mw	0.61

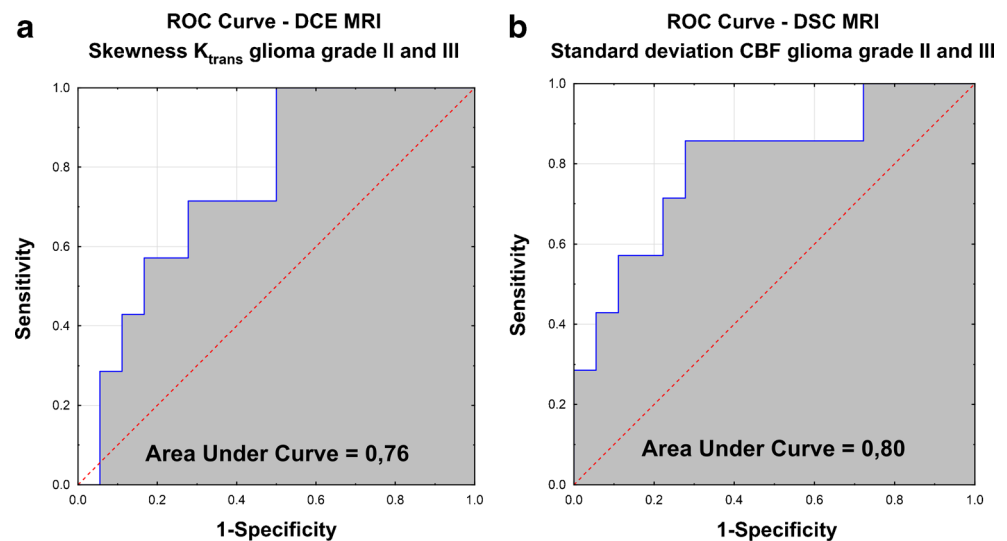
Statistically significant values are presented in bold font

*mw* Mann–Whitney *U* test, *tt* Student's *t* test

Perfusion analysis of gliomas in clinical practice is mainly limited to visual interpretation of perfusion maps presenting the mean value of each parameter. None of our data concerning highest AUC were mean or median values

(Tables 2 and 3), and therefore, a histogram analysis of perfusion data allows for a deeper analysis of the perfusion distribution in the tumour that exceeds that of mean values [29]. For example, the skewness of the histogram tells us how

**Fig. 2** **a** ROC curve for glioma grades II and III, presenting the parameter with the highest AUC: skewness *K*<sub>trans</sub> (DCE). **b** ROC curve for glioma grades II and III, presenting the parameter with the highest AUC: standard deviation CBF (DSC)



a data set is skewed to either right or left when deviating from a normal probability distribution. The kurtosis of the data tells us how broad or narrow the peak of the curve is when deviating from a normal probability distribution.

Apart from the limited number of included patients, possible limitations of the present study are the risk of classification errors in histopathological diagnoses of tumour samples derived from biopsies [30] and the risk of partial volume effect influencing the data retained from the ROIs [31]. The limited number of patients in this study does not permit us to draw any firm conclusions about those perfusion parameters that were unable to separate between glioma grades II and III. These parameters could still be valuable to investigate in a larger cohort. Since the DCE sequence included four slices over the central part of the tumour, the peripheral zones were incompletely covered in 18 out of 25 patients, possibly explaining why the result of the AUC analysis for the DCE perfusion was somewhat lower (0.76) than for the DSC perfusion (0.80). The temporal resolution for DCE was set to not over- or underestimate the perfusion parameters. An absolute quantification of perfusion parameters was prioritised over whole brain coverage, why the images were positioned to cover as much of the tumours as possible [32]. A limitation to the DCE method as applied in this study would thus be the risk of excluding glioma areas of importance for diagnosis. To be able to assess DCE and DSC respectively without compromising either of the perfusion methods, we chose to include the four tumour slices in DCE and all available tumour data on DSC.

To summarise, the results of this study yield further insight into pre-operative tumour evaluation through histogram analysis of perfusion parameters from DCE and DSC and present parameters that potentially can be used for grading of suspected low-grade gliomas.

## Conclusion

The skewness of  $k_{\text{trans}}$  (from DCE) and the standard deviation of rCBF (from DSC) could most efficiently discriminate between grade II and grade III gliomas.

**Ethical standards and patient consent** We declare that all human studies have been approved by the Uppsala Ethics Committee and have therefore been performed in accordance with the ethical standards laid down in the 1964 Declaration of Helsinki and its later amendments. We declare that all patients gave informed consent prior to inclusion in this study.

**Acknowledgments** The authors would like to thank Lars Berglund, Statistician, Uppsala Clinical Research Center, Sweden, Monika Gelotte, Research Assistant, Uppsala University, Sweden, and Håkan Pettersson, IT Manager, Uppsala University, Sweden.

**Conflict of interest** We declare that we have no conflict of interest.

## References

- Louis DN, Ohgaki H, Wiestler OD, Cavenee WK, Burger PC, Jouvet A, Scheithauer BW, Kleihues P (2007) The 2007 WHO classification of tumours of the central nervous system. *Acta Neuropathol* 114(2): 97–109. doi:10.1007/s00401-007-0243-4
- Hartmann C, von Deimling A (2009) Molecular pathology of oligodendroglial tumors. *Recent Results Cancer Res* 171:25–49. doi:10.1007/978-1003-1540-31206-31202\_31202
- Walker C, Baborie A, Crooks D, Wilkins S, Jenkinson MD (2011) Biology, genetics and imaging of glial cell tumours. *Br J Radiol* 84(2):S90–106. doi:10.1259/bjr/23430927
- Fan GG, Deng QL, Wu ZH, Guo QY (2006) Usefulness of diffusion/perfusion-weighted MRI in patients with non-enhancing supratentorial brain gliomas: a valuable tool to predict tumour grading? *Br J Radiol* 79(944):652–658. doi:10.1259/bjr/25349497
- Law M, Yang S, Babb JS, Knopp EA, Golfinos JG, Zagzag D, Johnson G (2004) Comparison of cerebral blood volume and vascular permeability from dynamic susceptibility contrast-enhanced perfusion MR imaging with glioma grade. *AJNR Am J Neuroradiol* 25(5):746–755
- Cha S, Tihan T, Crawford F, Fischbein NJ, Chang S, Bollen A, Nelson SJ, Prados M, Berger MS, Dillon WP (2005) Differentiation of low-grade oligodendrogliomas from low-grade astrocytomas by using quantitative blood-volume measurements derived from dynamic susceptibility contrast-enhanced MR imaging. *AJNR Am J Neuroradiol* 26(2):266–273
- Ostergaard L (2005) Principles of cerebral perfusion imaging by bolus tracking. *J Magn Reson Imaging* 22(6):710–717
- Cha S, Knopp EA, Johnson G, Litt A, Glass J, Gruber ML, Lu S, Zagzag D (2000) Dynamic contrast-enhanced T2-weighted MR imaging of recurrent malignant gliomas treated with thalidomide and carboplatin. *AJNR Am J Neuroradiol* 21(5):881–890
- Sourbron S, Ingrisch M, Siefert A, Reiser M, Herrmann K (2009) Quantification of cerebral blood flow, cerebral blood volume, and blood–brain-barrier leakage with DCE-MRI. *Magn Reson Med: Off J Soc Magn Reson Med / Soc Magn Reson Med* 62(1):205–217. doi: 10.1002/mrm.22005
- Larsson HB, Hansen AE, Berg HK, Rostrup E, Haraldseth O (2008) Dynamic contrast-enhanced quantitative perfusion measurement of the brain using T1-weighted MRI at 3 T. *J Magn Reson Imaging* 27(4):754–762. doi:10.1002/jmri.21328
- Larsson HB, Courivaud F, Rostrup E, Hansen AE (2009) Measurement of brain perfusion, blood volume, and blood–brain barrier permeability, using dynamic contrast-enhanced T1-weighted MRI at 3 tesla. *Magn Reson Med: Off J Soc Magn Reson Med / Soc Magn Reson Med* 62(5):1270–1281. doi:10.1002/mrm.22136
- Caseiras GB, Chheang S, Babb J, Rees JH, Pecorelli N, Tozer DJ, Benton C, Zagzag D, Johnson G, Waldman AD, Jager HR, Law M (2010) Relative cerebral blood volume measurements of low-grade gliomas predict patient outcome in a multi-institution setting. *Eur J Radiol* 73(2):215–220. doi:10.1016/j.ejrad.2008.11.005
- Knopp EA, Cha S, Johnson G, Mazumdar A, Golfinos JG, Zagzag D, Miller DC, Kelly PJ, Kricheff II (1999) Glial neoplasms: dynamic contrast-enhanced T2\*-weighted MR imaging. *Radiology* 211(3): 791–798
- Law M, Yang S, Wang H, Babb JS, Johnson G, Cha S, Knopp EA, Zagzag D (2003) Glioma grading: sensitivity, specificity, and predictive values of perfusion MR imaging and proton MR spectroscopic imaging compared with conventional MR imaging. *AJNR Am J Neuroradiol* 24(10):1989–1998
- Hilario A, Ramos A, Perez-Nunez A, Salvador E, Millan JM, Lagares A, Sepulveda JM, Gonzalez-Leon P, Hernandez-Lain A, Ricoy JR (2012) The added value of apparent diffusion coefficient to cerebral blood volume in the preoperative grading of diffuse gliomas. *AJNR Am J Neuroradiol* 33(4):701–707. doi:10.3174/ajnr.A2846

16. Liu X, Tian W, Kolar B, Yeane GA, Qiu X, Johnson MD, Ekholm S (2011) MR diffusion tensor and perfusion-weighted imaging in pre-operative grading of supratentorial nonenhancing gliomas. *Neuro-Oncology* 13(4):447–455. doi:10.1093/neuonc/noq197
17. Khalid L, Carone M, Dumrongpisutikul N, Intrapirromkul J, Bonekamp D, Barker PB, Yousem DM (2012) Imaging characteristics of oligodendrogliomas that predict grade. *AJNR Am J Neuroradiol* 33(5):852–857. doi:10.3174/ajnr.A2895
18. Saito T, Yamasaki F, Kajiwara Y, Abe N, Akiyama Y, Kakuda T, Takeshima Y, Sugiyama K, Okada Y, Kurisu K (2012) Role of perfusion-weighted imaging at 3T in the histopathological differentiation between astrocytic and oligodendroglial tumors. *Eur J Radiol* 81(8):1863–1869. doi:10.1016/j.ejrad.2011.1804.1009, Epub 2011 May 1864
19. Bertsson SG, Falk A, Savitcheva I, Godau A, Zetterling M, Hesselager G, Alafuzoff I, Larsson E-M, Smits A (2013) Perfusion and diffusion MRI combined with <sup>11</sup>C-methionine PET in the pre-operative evaluation of suspected adult low-grade gliomas. *J Neuro Oncol* 114(2):241–249. doi:10.1007/s11060-013-1178-3
20. Tofts PS (1997) Modeling tracer kinetics in dynamic Gd-DTPA MR imaging. *J Magn Reson Imaging* 7(1):91–101
21. Boxerman JL, Schmainda KM, Weisskoff RM (2006) Relative cerebral blood volume maps corrected for contrast agent extravasation significantly correlate with glioma tumor grade, whereas uncorrected maps do not. *AJNR Am J Neuroradiol* 27(4):859–867
22. Ostergaard L (2005) Principles of cerebral perfusion imaging by bolus tracking. *J Magn Reson Imaging* 22(6):710–717. doi:10.1002/jmri.20460
23. Calamante F, Gadian DG, Connelly A (2003) Quantification of bolus-tracking MRI: improved characterization of the tissue residue function using Tikhonov regularization. *Magn Reson Med: Off J Soc Magn Reson Med / Soc Magn Reson Med* 50(6):1237–1247. doi:10.1002/mrm.10643
24. Young R, Babb J, Law M, Pollack E, Johnson G (2007) Comparison of region-of-interest analysis with three different histogram analysis methods in the determination of perfusion metrics in patients with brain gliomas. *J Magn Reson Imaging* 26(4):1053–1063. doi:10.1002/jmri.21064
25. Morita N, Wang S, Chawla S, Poptani H, Melhem ER (2010) Dynamic susceptibility contrast perfusion weighted imaging in grading of nonenhancing astrocytomas. *J Magn Reson Imaging* 32(4):803–808. doi:10.1002/jmri.22324
26. Lev MH, Ozsunar Y, Henson JW, Rasheed AA, Barest GD, Harsh GR, Fitzek MM, Chiocca EA, Rabinov JD, Csavoy AN, Rosen BR, Hochberg FH, Schaefer PW, Gonzalez RG (2004) Glioma tumor grading and outcome prediction using dynamic spin-echo MR susceptibility mapping compared with conventional contrast-enhanced MR: confounding effect of elevated rCBV of oligodendrogliomas [corrected]. *AJNR Am J Neuroradiol* 25(2):214–221
27. Cha S, Yang L, Johnson G, Lai A, Chen MH, Tihan T, Wendland M, Dillon WP (2006) Comparison of microvascular permeability measurements, K(trans), determined with conventional steady-state T1-weighted and first-pass T2\*-weighted MR imaging methods in gliomas and meningiomas. *AJNR Am J Neuroradiol* 27(2):409–417
28. Hakyemez B, Erdogan C, Ercan I, Ergin N, Uysal S, Atahan S (2005) High-grade and low-grade gliomas: differentiation by using perfusion MR imaging. *Clin Radiol* 60(4):493–502. doi:10.1016/j.crad.2004.09.009
29. Emblem KE, Nedregaard B, Nome T, Due-Tonnessen P, Hald JK, Scheie D, Borota OC, Cvancarova M, Bjornerud A (2008) Glioma grading by using histogram analysis of blood volume heterogeneity from MR-derived cerebral blood volume maps. *Radiology* 247(3):808–817. doi:10.1148/radiol.2473070571
30. Scott CB, Nelson JS, Farnan NC, Curran WJ Jr, Murray KJ, Fischbach AJ, Gaspar LE, Nelson DF (1995) Central pathology review in clinical trials for patients with malignant glioma. A report of Radiation Therapy Oncology Group 83–02. *Cancer* 76(2):307–313
31. Battaglini M, Jenkinson M, De Stefano N (2012) Evaluating and reducing the impact of white matter lesions on brain volume measurements. *Hum Brain Mapp* 33(9):2062–2071. doi:10.1002/hbm.21344
32. Larsen VA, Simonsen HJ, Law I, Larsson HB, Hansen AE (2013) Evaluation of dynamic contrast-enhanced T1-weighted perfusion MRI in the differentiation of tumor recurrence from radiation necrosis. *Neuroradiology* 55(3):361–369. doi:10.1007/s00234-012-1127-4